

Short Communication

## Optimization of the nozzle structure for enhanced wear resistance of Ni–P–ZrO<sub>2</sub> composite coating prepared by jet electrodeposition

Na-na Ren, Mo-qi Shen, Wen-ke Ma, Shuang-lu Duan, Lan-ying Ding\*

College of Engineering, Nanjing Agricultural University, Nanjing 210095, China;

\*E-mail: [dinglying@njau.edu.cn](mailto:dinglying@njau.edu.cn)

Received: 19 April 2020 / Accepted: 29 June 2020 / Published: 10 August 2020

---

To reinforce the wear resistance of a rotary body, we prepared Ni–P–ZrO<sub>2</sub> composite coatings on the workpiece surface by jet electrodeposition using a straight nozzle. We observed minor vibration of the straight nozzle during the experiment, which affects the stability of the flow field in the machining gap between the nozzle and the workpiece surface. To ascertain the cause of this phenomenon, we used COMSOL to construct a simulation model of the spraying of the plating solution into the machining gap through the internal flow channel of the straight nozzle. Further, we analyzed the variation in the flow velocity and pressure of the plating solution with changes in the internal flow channel structure of the straight nozzle. Based on the simulation results and related literature, we obtained an optimized trapezoidal nozzle design. We further conducted similar simulations using the trapezoidal nozzle. The results indicate that the variation in the flow velocity of the plating solution was more gradual and the pressure distribution in the flow field was more uniform. These characteristics are beneficial for retarding the vibration of the straight nozzle and enhancing the flow field stability in the machining gap. The average wear scar width and depth of the composite coatings prepared using the trapezoidal nozzle were 293.51 and 1.15 μm, respectively, which are smaller than those (327.66 μm and 3.20 μm, respectively) of the composite coating prepared using the straight nozzle.

---

**Keywords:** jet electrodeposition; flow field simulation; nozzle; structure optimization; wear resistance

### 1. INTRODUCTION

Rotary parts are widely applied in machinery, such as hydraulic piston rods, engine pistons, roller bearing, and various shaft parts [1]. These parts operate under processes involving reciprocation movement or rotation and often in harsh working environments such as under high temperature, high pressure, heavy load, high-speed movement, and poor lubrication [2]. Therefore, these parts must possess excellent wear resistance. However, ordinary processing technology cannot meet such as a high

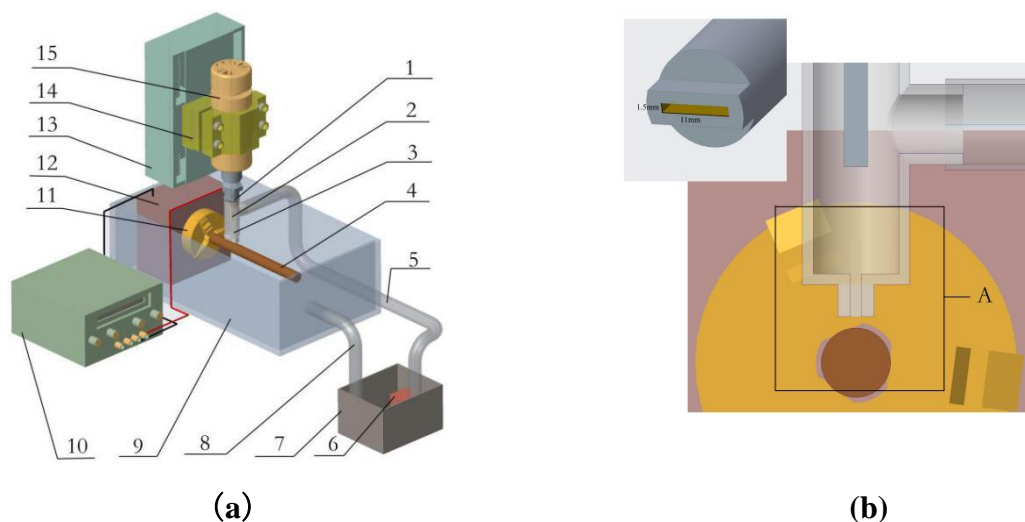
requirement. Jet electrodeposition, as a common surface modification technology, significantly improves the mechanical and anti-friction properties by preparing a high-quality coating on the surface of the workpiece, thereby extending the service life of the parts. Compared with conventional electrodeposition, the coatings fabricated by jet electrodeposition exhibit better performance and quality, resulting in greater utilization and saving of materials [3-5]. Therefore, jet electrodeposition has gained considerable research attention in recent years. For example, the performance of the composite coatings has been analyzed by considering the composition or concentration and the spraying speed or temperature of the plating solution as variables [6-8]. While some researchers have added external auxiliary conditions such as pulse assisted [9], ultrasonic assisted [10], and magnetic field [11] to prepare the coatings using jet electrodeposition, others have studied the properties of different coating materials, such as Cu-Al<sub>2</sub>O<sub>3</sub> [12], Ni-P [13], Co-Cr<sub>3</sub>C<sub>2</sub> [14], and Ni-Co [15]. Among these materials, electroless Ni-P composite coatings have gained immense popularity and acceptance in recent years because they provide considerable improvement of the desirable qualities such as hardness, wear, and abrasion resistance [16, 17]. Nano-ZrO<sub>2</sub> is characterized by its excellent physicochemical properties such as extreme hardness, high melting point, thermal and chemical stability, and wear and corrosion resistance [18, 19]. In summary, most of the existing studies focus on the research of jet electrodeposition on plane surfaces rather than curved surfaces, such as a rotary body. A previous study has shown that the cathode workpiece rotation causes changes in the conditions of the jet electrodeposition surface below the nozzle, which prevents continuous, preferential deposition in certain areas [20].

The shape of the nozzle of a jet electrodeposition device greatly affects the flow field, so it is an important factor to be considered in the jet electrodeposition experiment of a rotary body [21, 22]. The uniformity of the distribution of the flow field affects the distribution of ions in the plating solution; subsequently, uneven ion distribution will lead to uneven electrodeposition, which in turn reduces the surface quality and wear resistance of the composite coating [23]. Therefore, the structural design of the nozzle is particularly critical. However, optimization of the nozzle structural design usually requires considerable experimental verification. In this study, we conducted an experiment on the preparation of Ni-P-ZrO<sub>2</sub> composite coatings on the surface of a rotary body by using a straight nozzle. We observed slight vibrations in the straight nozzle, which affected the stability of the flow field in the machining gap between the nozzle and the workpiece. In order to ascertain the leading cause of this phenomenon, we used COMSOL to construct simulation models for the spraying of the plating solution into the machining gap through the internal flow channel of the straight nozzle. Furthermore, we analyzed the variation in the flow velocity and pressure of the plating solution due to changes in the internal flow channel structure of the straight nozzle. Then, the nozzle structure was optimized, and a trapezoidal nozzle was developed. The simulation results obtained using the trapezoidal nozzle indicated not only a gradual variation in the flow velocity of the plating solution but also a more uniform pressure distribution in the flow field. These characteristics are beneficial in retarding the slight vibration of the straight nozzle and enhancing the stability of the flow field in the machining gap. Therefore, the Ni-P-ZrO<sub>2</sub> composite coatings prepared on the surface of the rotary body using a trapezoidal nozzle have high wear resistance. Thus, a trapezoidal nozzle structure is more suitable than a straight nozzle for jet electrodeposition.

## 2. EXPERIMENTAL

### 2.1. Experimental Principle

The experimental device used for jet electrodeposition on the surface of a rotary body is illustrated in Figure 1. As shown in the figure, an anode nickel rod is installed on a machine tool spindle, and a piston is connected to a nozzle and the anode nickel rod. A cathode workpiece is mounted on a three-jaw chuck driven by a stepper motor in the box. A nozzle-moving device facilitates precise motion of the nozzle. The plating solution is heated, and the plating solution temperature is controlled by a temperature control device. When a certain voltage is applied to the anode nickel rod and the cathode workpiece, the plating solution is pumped through the inlet tube, presses through the nozzle, and is sprayed onto the surface of the cathode workpiece at a certain speed. Furthermore, the anode and cathode in the flow field forms a circuit through the plating solution. Thus, jet electrodeposition will occur on the affected area of the cathode workpiece surface as the current passes through the plating solution. During jet electrodeposition on the surface of a rotary body, the plating solution flows into the tank through the outlet tube, thus achieving circulation of the plating solution. Figure 2 shows the microscopic models of the Ni-P-ZrO<sub>2</sub> composite coatings obtained by jet electrodeposition. The co-deposition of metal ions and nano-ZrO<sub>2</sub> is divided into two steps. First, under the action of the electric field, nano-ZrO<sub>2</sub> coated with cations is transported to the substrate (cathode) surface, indicating weak adsorption. A reduction reaction occurs on the cathode surface, and nano-ZrO<sub>2</sub> and metal ions are trapped in the coatings, exhibiting strong adsorption. Thus, co-deposition is achieved and the Ni-P-ZrO<sub>2</sub> composite coating is formed [24].



1-Piston, 2-Anode nickel rod, 3-Nozzle, 4-Cathode workpiece, 5-Inlet tube, 6-Pump, 7-Tank, 8-Outlet tube, 9-Electroplating tank, 10-Power source, 11-Three-jaw chuck, 12-Box, 13 and 14-Nozzle-moving device, 15-Machine tool spindle

**Figure 1.** Experimental device of jet electrodeposition

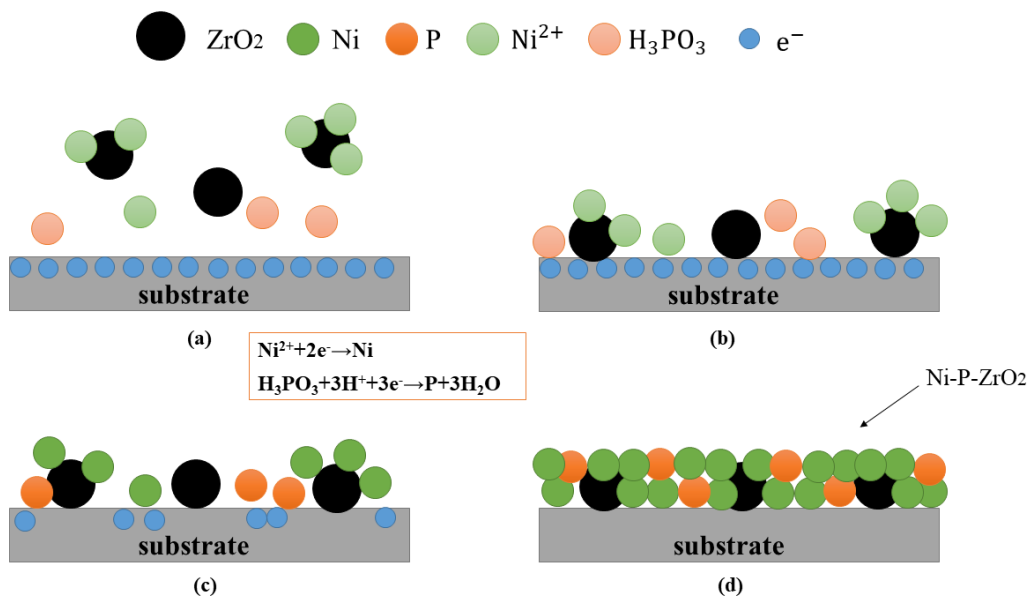


**Figure 2.** Microscopic model of the Ni–P–ZrO<sub>2</sub> composite coatings obtained by jet electrodeposition

### 2.2. Experimental setup

The workpiece used for the experiment is a 45 steel rotary body with dimensions  $\varnothing 10 \text{ mm} \times 70 \text{ mm}$ . Figure 3 shows the pretreatment process of the workpiece. Table 1 presents the composition of the plating solution, Table 2 lists the experimental process parameters, and Table 3 presents the details of the experimental instruments used and their application. Based on these specifications, we conducted an experiment of preparing the Ni–P–ZrO<sub>2</sub> composite coating using the jet electrodeposition device, shown in Figure 1 (a), with a straight nozzle of size  $1.5 \text{ mm} \times 11 \text{ mm}$ .

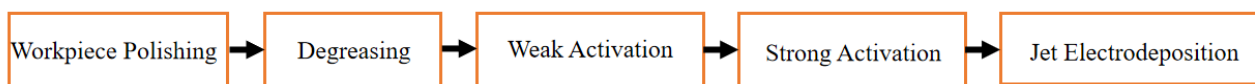


**Figure 3.** Pretreatment process of the workpiece

**Table 1.** Composition of the plating solution

Composition of the plating solution	Concentration (g/L)
NiSO <sub>4</sub> ·6H <sub>2</sub> O	200
NiCl <sub>2</sub> ·6H <sub>2</sub> O	30
H <sub>3</sub> PO <sub>3</sub>	20
H <sub>3</sub> BO <sub>3</sub>	30
C <sub>6</sub> H <sub>8</sub> O <sub>7</sub>	60
CH <sub>4</sub> N <sub>2</sub> S	0.01
C <sub>12</sub> H <sub>25</sub> SO <sub>4</sub> Na	0.08
nano-ZrO <sub>2</sub>	10

**Table 2.** Experimental process parameters

Experimental Process Parameters	Value
Voltage	25 V
Plating solution temperature	60 °C
Inlet velocity of plating solution	0.5 m/s
Cathode workpiece rotary speed	6 r/min
Relative motion speed of the nozzle	1500 mm/min
Processing time	60 min
ZrO <sub>2</sub> particle diameter	50 nm

**Table 3.** Experimental instrument and application

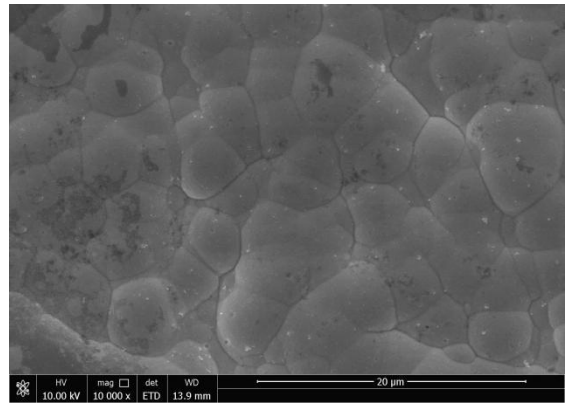
Experimental Instrument	Application
Scanning electron microscopy	Microscopic morphology
Laser confocal microscopy and OLS4100 program	Friction and wear diagrams of Ni–P–ZrO <sub>2</sub> composite coatings

### 3. RESULTS AND DISCUSSION

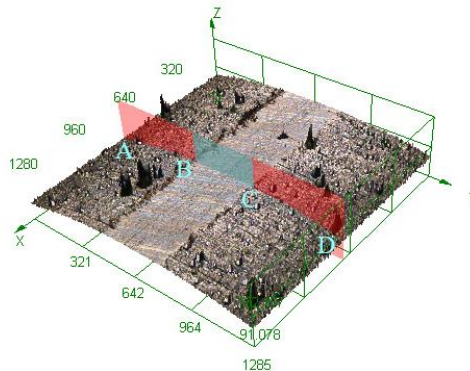
#### 3.1. Experimental Process and Result Analysis of the Straight Nozzle

In the experiment, we observed slight vibration of the straight nozzle when the plating solution was sprayed through the nozzle into the machining gap between the nozzle and the rotary body. The reason for the slight vibration of the straight nozzle can be attributed to the sudden external force acting on the nozzle [25]. Figure 1 (b) indicates that when the straight nozzle sprays the plating solution, due to the sudden change in the structure of the internal flow channel at point A, the plating solution flow is blocked, resulting in a sudden increase in the pressure it receives, which in turn causes the vibration of the straight nozzle.

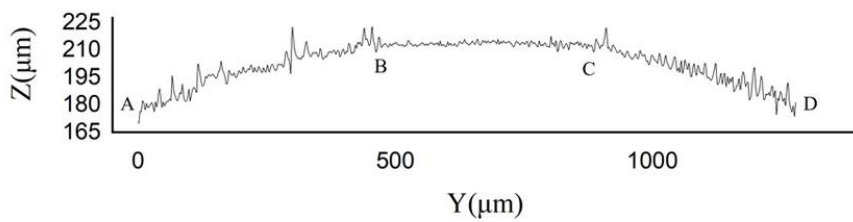
After the electrodeposition experiment, the surface morphology and wear resistance of the composite coatings were studied. Figure 4 (a) shows the scanning electron microscopy (SEM) morphology and the friction and wear diagrams of the Ni–P–ZrO<sub>2</sub> composite coatings prepared using the straight nozzle on the rotary body surface. Figure 4(a) indicates that the composite coating surface is relatively flat and the cells are arranged in a dense manner, but the cell boundary is tortuous and obvious. This could be because the slight vibration of the straight nozzle affects the distribution of the flow field, which in turn directly affects the quality and performance of the composite coating [24]. In the above experiment, the amount of friction and wear are indexes that directly reflect the wear resistance of the composite coating. Therefore, we used laser confocal microscopy and OLS4100 program to determine the wear width and depth for analyzing the wear resistance of the composite coating. Figure 4(b) and (c) show the friction and wear diagrams of the Ni–P–ZrO<sub>2</sub> composite coating prepared by the straight nozzle on the surface of the rotary body. In the diagrams, sections AB and CD represent the circular arcs on the surface of the rotary body, and section BC denotes the friction scars. Table 4 shows the measurement results of the wear parameters of the composite coatings.



(a)



(b)



(c)

**Figure 4.** (a) SEM surface morphology and (b, c) friction and wear diagrams of the Ni–P–ZrO<sub>2</sub> composite coating prepared with the straight nozzle on the surface of the rotary body.

**Table 4.** Measurement results of the wear parameters of the composite coatings obtained using the straight nozzle

Composite Coatings Properties	Number of Measurements					Average Value
	1	2	3	4	5	
Wear Width (μm)	333.94	326.40	332.68	327.66	317.62	327.66
Wear Depth (μm)	2.08	4.82	2.12	3.23	3.76	3.20

### 3.2. Simulation of a Straight Nozzle

To analyze the reason for the slight vibration of the straight nozzle and to alleviate the vibration, the flow field simulation of the experiment process was conducted. Using COMSOL, we constructed simulation models for the spraying of the plating solution into the machining gap through the internal flow channel of the straight nozzle. Due to the obvious change in the internal flow channel structure at point A in Figure 1(b), we mainly analyzed the characteristics of the flow field at this point. The variation in the flow velocity and pressure of the plating solution at A was analyzed, and the structure of the straight nozzle was optimized on this basis. Figure 5 shows a simplified diagram of the flow field simulation model area, wherein  $\tau_1$  represents the plating solution inlet boundary,  $\tau_3$  and  $\tau_6$  represent the plating solution outlet boundary,  $\tau_2$  and  $\tau_7$  represent the nozzle surface,  $\tau_4$  represents the nozzle exit surface, and  $\tau_5$  represents the cathode workpiece surface.

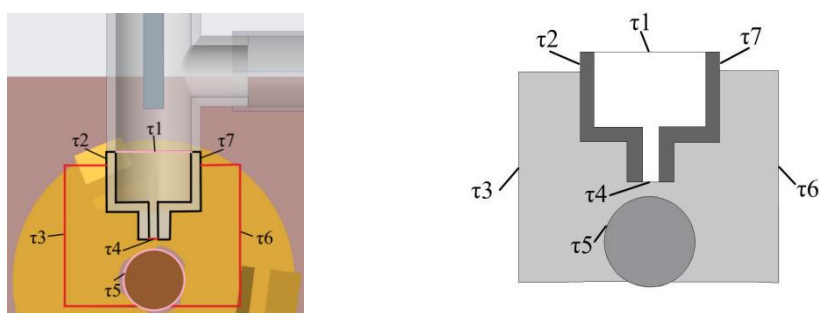


**Figure 5.** Simplified diagram of the flow field simulation model area

The flow velocity of the plating solution is one of the vital parameters affecting the jet electrodeposition process [26]; In addition, the stability and uniformity of the flow field can directly affect the composite coating quality [24]. When the plating solution is in a turbulent state, the flow velocity is higher and the circulation capacity is stronger, which allow timely replenishment of the ions consumed in the deposition process and transport of the reaction products of the machining gap; these phenomena are conducive to the smooth electrodeposition process. When the Reynolds number of the solution is greater than the lower critical Reynolds number (approximately 2320), the solution is turbulent. The Reynolds number is calculated as follows [27] :

$$R_e = \frac{Vd_H}{\nu} \quad (1)$$

where  $R_e$  is the Reynolds number,  $V$  is the average velocity of the section,  $d_H$  is the hydraulic diameter of the flow section, and  $\nu$  is the kinematic viscosity of the fluid. The calculation indicates that when the flow velocity of the plating solution to the inlet was higher than  $V = 0.36$  m/s, the plating solution flowing to the simulation area was turbulent. Therefore, because the flow velocity was set to 0.5 m/s in the experiment, the plating solution was turbulent. Thus, the following formula (2) (3) was applied to analyze the characteristics of the flow field.

To simplify the calculation, the following assumptions were made for the plating solution :

(1) The plating solution is a continuous incompressible viscous fluid free of bubbles and other impurities.

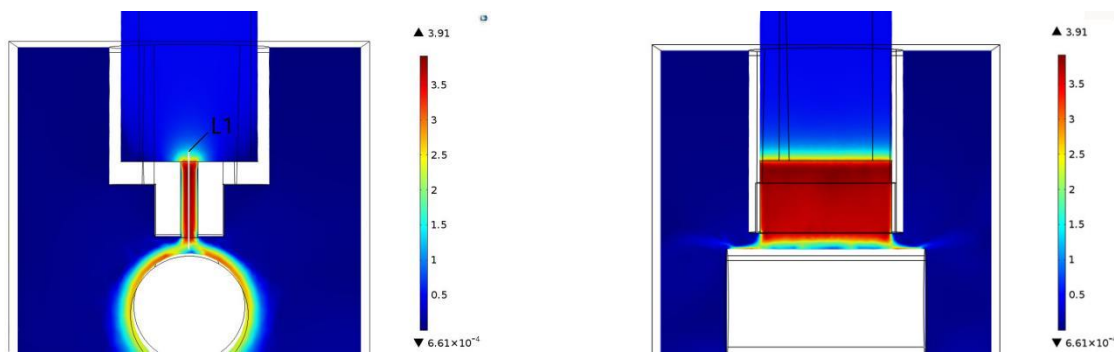
(2) The temperature changes and energy loss during the experiment are ignored.

Based on the above assumptions, and applying the laws of conservation of energy, mass, and momentum, the continuity equations and Navier–Stokes equations of fluid flow can be obtained as follows [27, 28]..

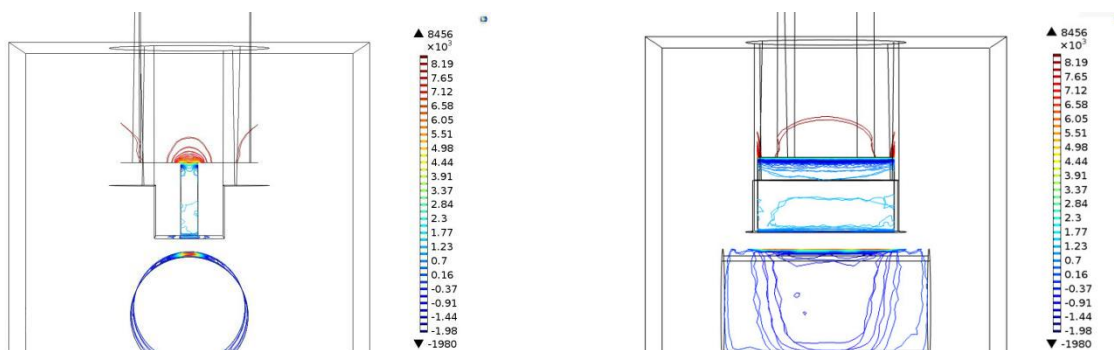
$$\frac{\partial u}{\partial x} + \frac{\partial v}{\partial y} + \frac{\partial w}{\partial z} = 0 \quad (2)$$

$$\rho \frac{dV}{dt} = \rho F - gradp + \mu \nabla^2 V \quad (3)$$

Here,  $u$ ,  $v$ , and  $w$  are the velocities along the  $x$ -,  $y$ -, and  $z$ -directions, respectively;  $\rho$  is the density of the plating solution;  $F$  is the volume force;  $p$  is the pressure on the fluid micro-body; and  $\mu$  is the dynamic viscosity of the plating solution. We solve equations (2) and (3) and use COMSOL to simulate the flow process of the plating solution sprayed into the machining gap through the internal flow channel of the straight nozzle, as shown in Figure 6.



(a) Flow velocity diagram of the straight nozzle flow field



(b) Pressure diagram of the straight nozzle flow field

**Figure 6.** Flow field simulation results of the straight nozzle

Figure 6 (a) shows the flow velocity diagram of the straight nozzle flow field. The figure indicates that even when the plating solution is not sprayed out, it has a stable flow velocity and uniform flow



field distribution. Conversely, when the flow path structure of the straight nozzle changes, the flow velocity at the center increases sharply, disrupting the flow field stability. As the plating solution reaches the surface of the rotary body, the flow velocity decreases. Figure 6 (b) shows the pressure diagram of the straight nozzle flow field, and it indicates that the pressure distribution curve under the flow field is dense and depends on the changes in the flow channel structure of the straight nozzle. However, on the inner wall of the nozzle outlet, the pressure on the straight nozzle is weak. After the plating solution flows out, the pressure concentrates on the top of the upper surface of the rotary body.

The above experiments and simulations demonstrate that during the jet electrodeposition process, the flowing plating solution causes a vibration of the straight nozzle, which would lead to wear on the nozzle over time. If the wear is severe, the nozzle will be damaged and the wear resistance of the composite coatings will be adversely affected. To avoid the loss caused by nozzle failure, a general method is to increase the nozzle wall thickness or use a strong and expensive nozzle material [29]. Although this can increase the nozzle life to a certain extent, the cost is higher and the straight nozzle vibration phenomenon caused by the changes of the internal flow channel structure cannot be eliminated entirely. Therefore, it is necessary to optimize the nozzle structure.

### 3.3. Design Optimization

To alleviate the slight vibration of the straight nozzle caused by the sudden increase in the flow velocity of the plating solution and the concentration of pressure, the internal flow channel structure must be optimized. When the nozzle configuration is changed, the flow of the plating solution inside the nozzle changes, possibly resulting in different flow characteristics of the plating solution from the nozzle exit, which directly affects the composite coating performance [30]. The optimized nozzle internal flow channel should avoid sudden changes in the channel structure so as to reduce the change rate of the flow velocity and the local high stress. Therefore, the nozzle with a trapezoidal channel structure was developed, that is, a trapezoidal nozzle. The upper port of the trapezoidal nozzle is 4 mm and the lower port is 1.5 mm. The other dimensions are the same as those of the straight nozzle. Figure 7 shows a sectional view of a trapezoidal nozzle. Using COMSOL, we performed the simulation of the flow process of the spraying of the plating solution into the machining gap through the internal flow channel of the trapezoidal nozzle.

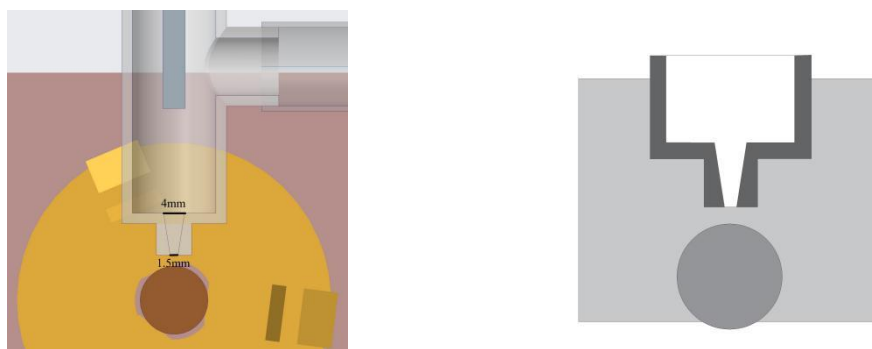
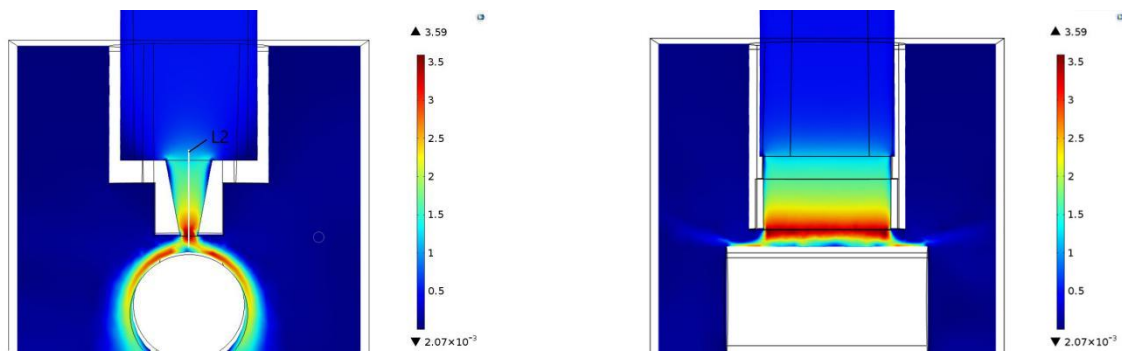
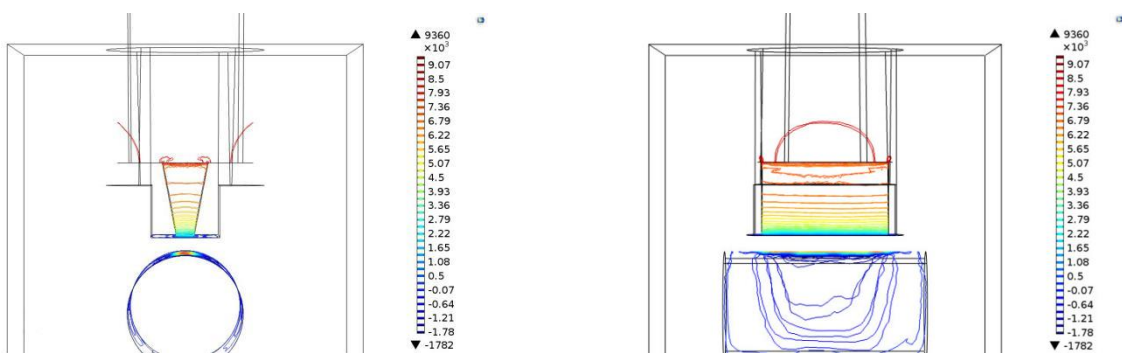


**Figure 7.** Sectional view of a trapezoidal nozzle

3.4. Simulation of a Trapezoidal Nozzle



(a) Flow velocity diagram of the trapezoidal nozzle flow field



(b) Pressure diagram of the trapezoidal nozzle flow field

**Figure 8.** Flow field simulation results of the trapezoidal nozzle

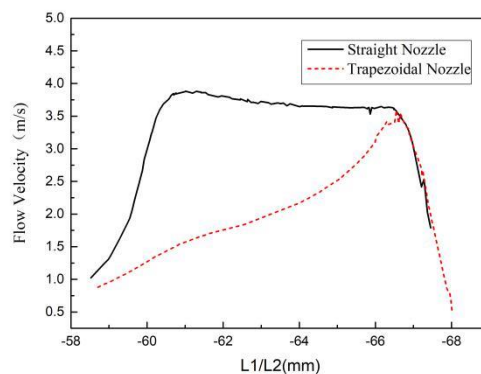


**Figure 9.** Flow velocity changes of the straight and trapezoidal nozzles in the L1 and L2 directions

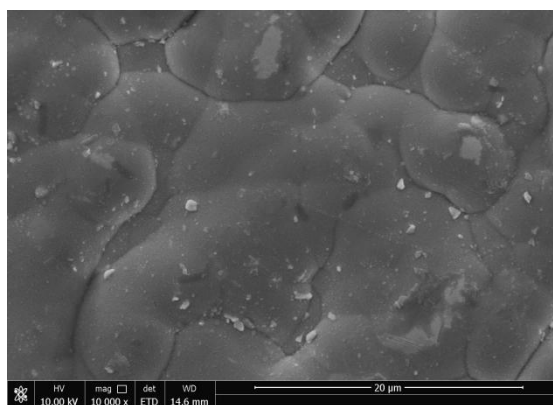
We imported the COMSOL-generated flow field model of preparing Ni-P-ZrO<sub>2</sub> composite coatings using the trapezoidal nozzle on the surface of the rotary body, keeping the same boundary conditions as those for the straight nozzle simulation. The flow process simulation result of the plating solution injected into the machining gap through the internal flow channel of the trapezoidal nozzle is shown in Figure 8.

The flow velocity diagram of the trapezoidal nozzle flow field (Figure 8(a)) indicates that until the plating solution reaches the structural change point, the flow velocity distribution is uniform and the

flow field is stable. With the change in the structure, the flow velocity of the plating solution increases gradually compared to the straight nozzle and it reaches the maximum value at the nozzle outlet. The pressure diagram of the trapezoidal nozzle flow field (Figure 8(b)) shows that the pressure distribution of the plating solution in the trapezoidal nozzle is more uniform than in the straight nozzle; thus, the phenomenon of pressure concentration is avoided, which is conducive to reducing the vibration of the nozzle and improving the stability of the flow field. Figure 9 shows the flow velocity changes of the two types of nozzles in the L1 and L2 directions, as shown in Figures 6 (a) and 8 (a). The figure indicates that the change in flow velocity of the trapezoidal nozzle in the L2 direction is lower than that of the straight nozzle in the L1 direction.

### 3.5. Experimental Process and Result Analysis of the Trapezoidal Nozzle

Using the same process parameters as those of the straight nozzle experiment, a trapezoidal nozzle with a size of 1.5 mm × 11 mm was used to conduct the experiment of preparing Ni–P–ZrO<sub>2</sub> composite coatings on the surface of a rotary body. No vibration of the trapezoidal nozzle was observed in the experiment, indicating that the pressure concentration was relieved. The SEM morphology of the Ni–P–ZrO<sub>2</sub> composite coating prepared with the trapezoidal nozzle on the surface of the rotary body is shown in Figure 10(a). It indicates the Ni–P–ZrO<sub>2</sub> composite coating surface is dense and flat, the structure is compact, and the boundary is extremely blurred. This is because the flow velocity in the trapezoidal nozzle is stable and uniform, which reduces the concentration difference caused by the rapid change in the flow velocity. Thus, a uniform distribution of the cathode workpiece ions and nano-ZrO<sub>2</sub> on the surface is achieved, thereby improving the composite coating performance [31, 32]. Figures 10 (b) and (c) show the friction and wear diagrams of the Ni–P–ZrO<sub>2</sub> composite coatings on the surface of the rotary body using the trapezoidal nozzle. Table 5 shows the measurement results of the wear parameters of the composite coatings. Compared with the wear parameters obtained with the straight nozzle, the composite coatings obtained with the trapezoidal nozzle had a smaller wear scar width and approximately half the wear scar depth. These results can be attributed to the higher density and smoother surface of the composite coating produced by the trapezoidal nozzle. Consequently, the wear resistance of the Ni–P–ZrO<sub>2</sub> composite coating prepared on the surface of the rotary body with the trapezoidal nozzle is superior.



(a)

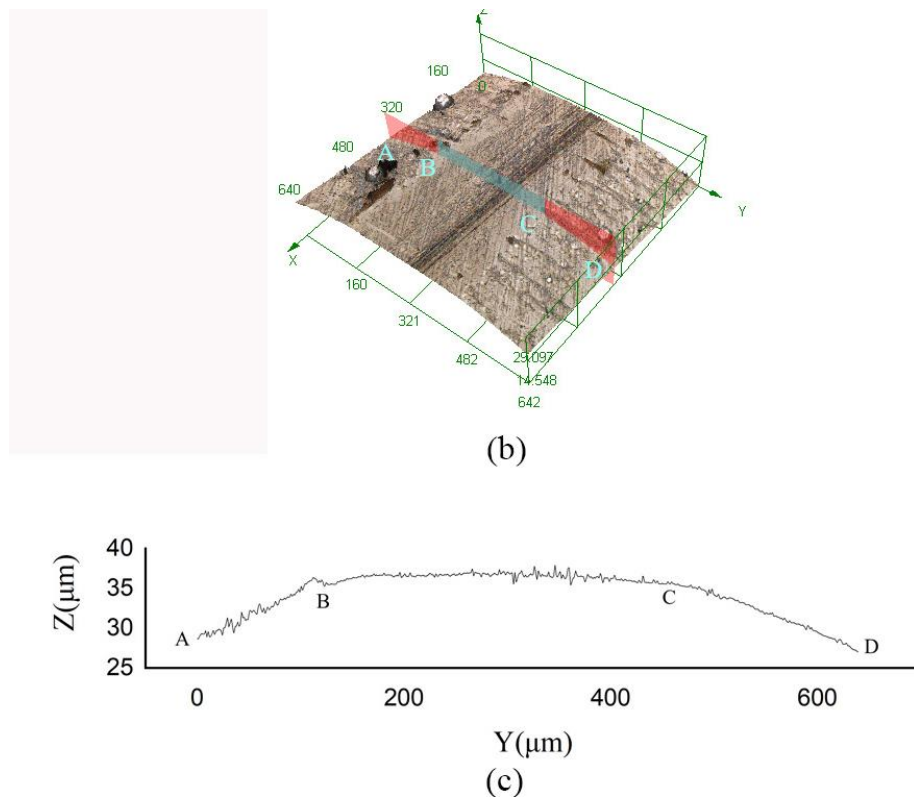


**Figure 10.** (a) SEM surface morphology and (b, c) friction and wear diagrams of the Ni-P-ZrO<sub>2</sub> composite coating prepared using the trapezoidal nozzle on the surface of the rotary body

**Table 5.** Measurement results of the wear parameters of the composite coatings obtained with the trapezoidal nozzle

Composite Coatings Properties	Number of Measurements					Average Value
	1	2	3	4	5	
Wear Width (μm)	298.78	293.76	278.07	298.78	298.16	293.51
Wear Depth (μm)	1.81	0.78	0.96	1.18	1.02	1.15

#### 4. CONCLUSION

In this study, to reinforce the wear resistance of rotary parts, an experimental study was conducted on the preparation of Ni-P-ZrO<sub>2</sub> composite coatings on the surface of a rotary body using the jet electrodeposition process with a straight nozzle. The results indicated the occurrence of minor vibration of the straight nozzle during the electrodeposition process. In addition, the composite coating

surface produced with the straight nozzle was convex and rough. Using laser confocal microscopy and the OLS4100 program, the wear width and depth of the composite coatings were determined as 327.66 and 3.20  $\mu\text{m}$ , respectively.

To reduce the vibration of the straight nozzle, COMSOL was used to simulate a flow field model of preparing Ni–P–ZrO<sub>2</sub> composite coatings on the rotary body surface. The results indicated that the flow velocity of the plating solution changes sharply and the pressure on the plating solution suddenly increases with changes in the internal flow channel structure of the straight nozzle. This disrupts the stability of the flow field and degrades the quality of the Ni–P–ZrO<sub>2</sub> composite coating.

Based on the above phenomenon, the straight nozzle structure was optimized to obtain a trapezoidal nozzle. The same simulation and experiments were performed using the trapezoidal nozzle. The results showed that, compared with the straight nozzle, the change in the flow velocity of the plating solution in the trapezoidal nozzle was gradual and the pressure distribution in the flow field was more uniform. Thus, the nozzle vibration could be reduced and the stability of the flow field in the machining gap was improved. At the same time, the surface of the Ni–P–ZrO<sub>2</sub> composite coating obtained with the trapezoidal nozzle was relatively flat. The wear scar width and depth were 293.51 and 1.15  $\mu\text{m}$ , respectively; these values are, respectively, smaller and nearly half the wear parameter values obtained using the straight nozzle. Therefore, the Ni–P–ZrO<sub>2</sub> composite coatings prepared on the surface of the rotary body using a trapezoidal nozzle have high wear resistance. Thus, a trapezoidal nozzle structure is more suitable than a straight nozzle for jet electrodeposition.

#### ACKNOWLEDGEMENTS

Financial support for this work was provided by the Innovation and Entrepreneurship Training Program for College Students of Nanjing Agricultural University (1930C13).

#### References

1. H. Jin, T. Avitus, Y. Liu, Y. Wang, Han, Y. Zheng, *Sensors (Basel, Switzerland)*, 19 (2019) 4069.
2. J. Jin, X. Wang, L. Li, *Journal of Mechanical Science and Technology*, 30 (2016) 2723.
3. D. Ning, A. Zhang, H. Wu, *Materials (Basel, Switzerland)*, 12 (2019) 392.
4. Y. Wang, M. Kang, C. Chen, Y. Yang, X. Fu, *Nongye Gongcheng Xuebao/Transactions of the Chinese Society of Agricultural Engineering*, 29 (2013) 48.
5. Y. Wang, M. Kang, X. Fu, X. Wang, *Nongye Gongcheng Xuebao/Transactions of the Chinese Society of Agricultural Engineering*, 30 (2014) 54.
6. L. Ji, F. Chen, H. Huang, X. Sun, Y. Yan, X. Tang, *Surface & Coatings Technology*, 351 (2018) 212.
7. H. Wang, Y. Dou, Q. Fu, K. Tan, *Corrosion Science & Protection Technology*, 26 (2014) 307.
8. J. Yu, J. Zhao, M. Yu, H. Luo, Q. Qiao, S. Zhai, Z. Xu, K. Matsugi, *Bulletin of Materials Science*, 41(2018) 41.
9. F. Xia, W. Jia, M. Jiang, W. Cui, J. Wang, *Ceramics International*, 43 (2017) 14623.
10. M. Rajput, *Proceedings of the institution of mechanical engineers part b journal of engineering manufacture*, 228 (2014) 682.
11. W. Jiang, L. Shen, M. Qiu, X. Wang, M. Fan, Z. Tian, *Journal of Alloys and Compounds*, 762 (2018) 115.

12. H. Fan, Y. Zhao, S. Wang, H. Guo, *The International Journal of Advanced Manufacturing Technology*, 105 (2019) 4509.
13. M.I. Ansaria , D.S.G. Thakura, *Materials Today: Proceedings*, 4 (2017) 9870.
14. X.H. Zheng, M. Wang, H. Hao, D. Liu, X.T. Liu, J.Tang, *Surface and Coatings Technology*, 325 (2017) 181.
15. M. Kang, Y. Zhang, H.Z. Li, *Procedia CIRP*, 68 (2018) 221.
16. J.N. Balaraju, T.S.N. Sankara Narayanan, S.K. Seshadri, *Journal of Solid State Electrochemistry*, 5 (2001) 334.
17. D. R.Dhakala, G. Gyawalib, Y.K. Kshetric , J.H. Choia , S.W. Leea, *Surface and Coatings Technology*, 381 (2020) 125135.
18. E .Beltowska-Lehman, A. Bigos, M.J. Szczerba, M.J anusz-Skuza, L. Maj, A. Debski, G. Wiazania, M. Kot, *Surface and Coatings Technology*, 393 (2020) 125779.
19. E. Beltowska-Lehman, P. Indyka, A. Bigos, M.J. Szczerba, M. Kot, *Materials and Design*, 80(2015)1
20. C.Wang, L.D. Shen, M.B. Qiu, Z.J. Tian, W.Jiang, *Journal of Alloys and Compounds*, 727 (2017) 269.
21. P. Sun, L. Song. Influence Analysis on Inner Flow Field of Nozzle for Different Radius and Shapes of Pintle[P]. Information Engineering and Computer Science, 2009. ICIECS 2009. International Conference on,(2009), 1.
22. Y. Lei, R. Wang, D. Jiang, K. Liu, P. Tang, Simulation and analysis of flow field in abrasive water jet nozzle[P]. Consumer Electronics, Communications and Networks (CECNet), 2011 International Conference on,(2011), 5219.
23. Rajput M S, Pandey P M, Jha S, *International Journal of Advanced Manufacturing Technology*, 76 (2013) 61.
24. W.Jiang , L.D. Shen , M.Y. Xu, Z.W. Wang, Z.J. Tian, *Journal of Alloys and Compounds*. 791 (2019) 847.
25. Y. Chen, *China equipment engineering*, 12 (2018) 88.
26. H. Kim, J.G. Kim, J.W. Park, C.N. Chu, *Precision Engineering*, 51 (2018) 153.
27. W. Graebel, A. Paintal, *Applied Mechanics Reviews*,54 (2011) 89.
28. E. Jhon Finnemore, Joseph B, Frazini. Fluid Mechanics and Engineering Applications, Tsinghua University Press, (2004), Beijing, China.
29. R. Shi, M. Li, B. Wang, B. Zhang, X. Li, *Hot Processing Technology*, 43 (2014) 121.
30. Y. Liu, J. Zhang, J.P. Wei, X.T. Liu, *Power Technology*, 364 (2020) 343.
31. T. Pérez, L.F. Arenas, D. Villalobos-Lara, N. Zhou, S.C. Wang, F.C. Walsh, J. L Nava, C.P.D. León, *Journal of Electroanalytical Chemistry*, (2020) 114359
32. F.C. Walsh, S.C. Wang, N. Zhou, *Current Opinion in Electrochemistry*, 20 (2020) 8.